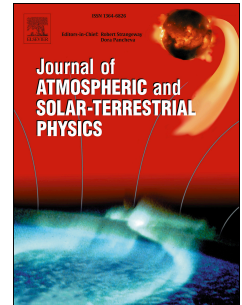


Accepted Manuscript

Characterization of ionospheric irregularities at different longitudes during quiet and disturbed geomagnetic conditions

O.S. Bolaji, S.J. Adebisi, J.B. Fashae



PII: S1364-6826(18)30344-4

DOI: <https://doi.org/10.1016/j.jastp.2018.11.007>

Reference: ATP 4953

To appear in: *Journal of Atmospheric and Solar-Terrestrial Physics*

Received Date: 22 May 2018

Revised Date: 11 November 2018

Accepted Date: 19 November 2018

Please cite this article as: Bolaji, O.S., Adebisi, S.J., Fashae, J.B., Characterization of ionospheric irregularities at different longitudes during quiet and disturbed geomagnetic conditions, *Journal of Atmospheric and Solar-Terrestrial Physics* (2018), doi: <https://doi.org/10.1016/j.jastp.2018.11.007>.

This is a PDF file of an unedited manuscript that has been accepted for publication. As a service to our customers we are providing this early version of the manuscript. The manuscript will undergo copyediting, typesetting, and review of the resulting proof before it is published in its final form. Please note that during the production process errors may be discovered which could affect the content, and all legal disclaimers that apply to the journal pertain.

Characterization of ionospheric irregularities at different longitudes during quiet and disturbed geomagnetic conditions.

O.S. Bolaji^{a,b}, S.J. Adebisi^{c*}, J.B. Fashae^d

^a*Department of Physics, University of Lagos, Lagos, Nigeria.*

^b*Department of Physics, University of Tasmania, Hobart, Australia.*

^c*Department of Physics, Landmark University, Omu-Aran, Nigeria.*

^d*Department of Physical Sciences, Bells University of Technology, Ota, Nigeria.*

*Corresponding Author: (johndat2003@gmail.com; adebiyi.shola@lmu.edu.ng; +234 703 0880 504)

Abstract

This paper investigates the plasma irregularities at different longitudes in the month of March 2015; a period that consists of both quiet and disturbed geomagnetic conditions. The average rate of change of TEC index (ROTI_{ave}), derived from Global Positioning System (GPS) measurements obtained at South America, Africa, Asia and Oceania equatorial regions, was used as indicator. The observations revealed significant longitudinal differences for both quiet and disturbed conditions. The quiet-time observations indicate that irregularities were most frequent in the American and African sectors, it is rarely observed in the Asian sector and mostly absent in the Oceania longitudes. The strength is however observed to decrease eastward i.e. it is most prominent in the American sector (up to ~1.6 TECU/min.) and absent in the Oceania longitudes. The results of the investigation of the 17 March, 2015 storm event revealed that the storm appeared not to hinder the development of irregularities in all the stations in the America sector during the night following the main phase. However, significant longitudinal variation is observed within the sector on the first night following the storm's recovery. In the African sector, the storm inhibits the development of irregularities in all the stations during the storm days considered: a development that is fundamentally different from the America sector. Generally, no significant storm effect is observed in the Asian and Oceania stations considered. The storm-time longitudinal variations of irregularities have been partly attributed to the storm timing and significant longitudinal difference in the action of storm-induced related drivers.

Keywords: Irregularities; ROTI; Scintillation; Geomagnetic storm.

1. Introduction

The ionized portion of the earth's upper atmosphere sometimes becomes unstable and develops plasma density irregularities. These irregularities in the ionosphere scatter radio waves in the frequency range of 100 MHz–4 GHz (Basu et al., 1988; Aarons, 1993; Aarons and Basu, 1994) causing rapid fluctuation in the intensity and phase of radio signal; a process known as ionospheric scintillations. Ionospheric scintillations mainly occur around the equatorial region essentially at night, shortly after local sunset and are associated with the Rayleigh-Taylor and F2 layer plasma drift instabilities. The presence of irregularities in the ionosphere are believed to be the primary source of ionospheric scintillation. Ionospheric scintillation degrades trans-ionospheric signals, resulting in signal fading below the fade margin of the receiver, and leading to the signal loss and cycle slips (Kintner et al. 2007; Tanna and Pathak 2014).

Many observation techniques such as the digisonde, the GPS, optical imager and many more have been employed to study the ionospheric irregularities at different regions and report of the investigations have been documented (e.g. Abdu et al., 1981; Hysell and Burcham, 1998; Su et al., 2008; Lynn et al., 2011). For examples, the investigations by Woodman and LaHoz (1976), Yeh and Liu (1982), Basu

and Basu (1985), Muella et al. (2009) and many others have shown that the occurrence of irregularities depends on local time, season, latitude, solar cycle and magnetic activity. Basu et al. (1988) reported a maximum occurrence of scintillation during the high solar activity period. They also found that irregularities/scintillations were most pronounced around the equatorial ionization anomaly (EIA); a region on both sides of the dip equator (about $\pm 15^\circ$) where the highest electron content and gradients are found to exist. Also, Muella et al. (2009) found that on geomagnetically disturbed nights, scintillation activities seemed to be strongly affected by the penetration of magnetospheric electric fields.

The occurrence of geomagnetic storm may trigger various physical processes which affect the plasma dynamics and may alter the background ionospheric morphology. The disturbance may enhance or impede the evolution of ionospheric irregularities, particularly at the equatorial region, with a consequent effect on scintillations of radio signals. Several studies had been conducted to examine the effect of geomagnetic storm on the occurrence of ionospheric irregularities at different sectors of the world (e.g. Aarons, 1991; Basu et al., 2001; Biktash et al., 2004; Chu et al., 2005; Li et al., 2006; Campos de Rezende et al., 2007; Li et al., 2008; Oladipo and Schüler et al., 2012, 2013; Ngwira et al., 2013; Deng et al., 2015). For example, Aarons et al. (1997) reported a modification in the diurnal pattern of irregularities during geomagnetic storm event over the American equatorial region. Such modification in the pattern of ionospheric irregularities was reported by Oladipo and Schuler (2013) over the African sector. They found that the occurrence of irregularities is affected by the local time of the storm's main phase.

A number of studies has investigated the effect of the 17 March, 2015 geomagnetic storm event on the dynamics of the ionosphere at different locations many of which have been reported in special issues in some journals (e.g. Zhang et al., 2015; Yadav et al., 2016; Rajesh et al., 2017; Hairston et al., Huang et al., 2016; Kuai et al., 2016 Lyons et al., 2016; Huba et al., 2016; Kil et al., 2016; Patra et al., 2016; Zhou et al., 2016; Spogli et al., 2016; Ray et al., 2017; Borries et al., 2016; Nava et al., 2016; Ikubanni et al. 2018). Some of the area covered by these studies include modeling, observation, data and assimilation (see Zhang et al. 2017). In all the collections, Kil et al. (2016), Patra et al. (2016), Zhou et al. (2016), Spogli et al. (2016), Ray et al. (2017) and Rajesh et al. (2017) have investigated the low latitude ionospheric irregularities at different locations, mostly in the Asian longitudes. The aim of this paper is to investigate the longitudinal variation of ionospheric irregularities during this storm event. Simultaneous investigation at different longitudes under the same external condition may provide important information that are still relevant which may improve our current understanding on the physical mechanisms responsible for the development of irregularities at individual sector. In this study, we employed GPS data obtained receivers located in South American, African, Asian and Oceania equatorial and low latitude stations. Using the GPS technology has been considered ideal to study ionospheric irregularities and has provided a means to obtain a general pattern of global ionospheric irregularities distribution and its variability.

2. Data and Method of Analysis

Different observation techniques have been used to study the irregularities in the ionosphere. In this paper, the ionospheric irregularities during the period 01-31 March, 2015, comprising both quiet and disturbed periods, is investigated using the fluctuation index derived from the GPS measurements. The GPS data are the simultaneous measurements from the receivers located within the equatorial region in the South American, African, Asian and Oceania sectors. The receivers are all part of International

GNSS Service (IGS) network of receivers whose measurement are archived in Receiver INdependent EXchange (RINEX) format and are available at <ftp://geodaf.mt.asi.it/GEOD/GPSD/RINEX>. Table 1 shows the geophysical detailed of the data sites used for the investigation. We have used the GPS-TEC analysis software developed by Gopi Seemala of the Indian Institute of Geomagnetism to estimate the value of TEC from the GPS measurement. In our estimation, an elevation angle cut-off of 30^0 was adopted in other to eliminate the multipath effect on the measurements.

Many researchers have used different fluctuation indices to represent ionospheric irregularities. In this study, the Rate of change of the TEC index (ROTI) is employed. ROTI is a parameter derived from the time variation of TEC (i.e. rate of change of TEC (ROT) given by equation 1). Pi et al. (1997) calculated it, based on the standard deviation of ROT over a 5-minute period and is given by the expression in the equation 2

$$ROT = \frac{dTEC}{dt} \quad (1)$$

$$ROTI = \sqrt{\langle ROT^2 \rangle - \langle ROT \rangle^2} \quad (2)$$

Mendillo et al. (2000), using the expression in equation 3 computed the average ROTI ($ROTI_{ave}$) ($ROTI_{ave}$ is a good proxy that indicate the 30-minutes phase fluctuation level over a location.) as the average of ROTI over 30 min interval for a satellite and then the average over all satellites in view. This result gives the average level of irregularities (phase fluctuation) for half an hour over the station.

$$ROTI_{ave}(0.5h) = \frac{1}{nsat(0.5h)} \sum_n^{nsat} \sum_i^k \sum_i^k \frac{ROTI(n, 0.5h, i)}{k} \quad (3)$$

where n is the satellite number, h is hour (0, 0.5, 1, ..., 23.5, 24 UT), i is the 5 min section within half an hour ($i = 1, 2, 3, 4, 5$, and 6), nSat (0.5 h) is the number of satellites observed within half an hour, and k is the number of ROTI values available within half an hour for a particular satellite. Adopting the classification by Oladipo and Schüler (2013), the value of $ROTI_{ave} \geq 0.4$ TECU/min is considered to indicate the presence of background ionospheric irregularities in this investigation. Oladipo and Schüler (2013) had earlier categorized the values of $ROTI_{ave}$ as follows: $ROTI_{ave} < 0.4$ to indicate the absent of phase fluctuation activity, $0.4 < ROTI_{ave} < 0.8$ to indicate that there is phase fluctuation activity, and $ROTI_{ave} > 0.8$ to indicate severe phase fluctuation activity.

3. Results and discussion

3.1 Ionospheric irregularities during quiet condition

Figures 2 - 5 show the diurnal plots of the average rate of total electron content index ($ROTI_{ave}$) index over South America, Africa, Asia and Oceania region respectively for all the days in the month of March, 2015. The figures indicate that irregularities were largely present in most of the stations before, during and after the geomagnetic storm days particularly in the South American. The frequency of occurrence is higher at South America and African sectors and is less at the other two longitudes particularly over Oceania. The average behavior for ten quietest days of the month was further analyzed and the results presented in Fig. 6. The results of the analysis indicate that ionospheric irregularities show a significant longitudinal difference. Irregularities were observed in the South American and African sectors only and are generally registered between 19:00 LT -00:00 LT in most of the stations. The magnitude is generally found to decrease eastward during the quiet condition. In

other words, strength of the irregularities was found to be most severe in the South American sector (up to about 1.6 TECU/min.), rarely observed in the Asian sector and were absent over the Oceania.

Electric field due to E-region conductivity plays a significant role in plasma dynamic of the equatorial region. The electric field (E) in conjunction with the magnetic field (which about horizontal at the equatorial region) produces an $E \times B$ electrodynamics force that affect plasma distribution in the region. The direction of the force is such that it is upward (or downward) during the day (or night) when the electric field is eastward (or westward). In addition, the action of the F-region dynamo during the post-sunset hours enhances the daytime eastward electric field. This intensifies the upward motion of plasma during that periods to higher altitudes where the collision frequencies are low and hence lower recombination rate. The result is enhancement of the F-region electron density during that period (a phenomenon known as pre-reversal enhancement (PRE)). PRE have been reported to play an important role in the development of post-sunset ionospheric irregularities (Fejer et al., 1999). The upward density gradient between the topside F-region plasma lifted by the enhanced $E \times B$ force after sunset and the depleted bottom-side E-region plasma due to the absence of solar radiation creates plasma instability which give rise to ionospheric irregularities. This may account for the irregularities observed over South American and African longitudes between 19:00 LT -00:00 LT.

Large scale ionospheric irregularities are generated from diffusion of plasma from high ionospheric altitude (Ngwira, et al., 2013). Therefore, the eastward decrease in the strength of ionospheric irregularities may be an indication that it is either the magnitude of daytime eastward equatorial electrojet (EEJ) current reduces from west to east near the post-sunset hours or there is a daytime westward electric field (or counter EEJ) imposed on the normal daytime eastward field and which intensifies from east to west. More works may be required in this direction. Strong EEJ current may implies strong fountain effect (i.e. strong $E \times B$ plasma drift). Strong formation of $E \times B$ upward plasma drift may result into a sharp density gradient which may favor the development of large scale irregularities.

3.2 Ionospheric irregularities during the 17 March, 2015 geomagnetic storm.

The 17 March, 2015 is one of the most intense storm events in this present solar cycle (solar cycle 24) with SYM-H minimum value of -234 nT as shown in Fig. 7. The Figure also include from the upper panel to the bottom: the interplanetary magnetic field (IMF- B_z) and (IMF- B_y) components, the planetary Ap and Kp indices, the proton density (N_p), the solar wind speed (V_z), the symmetric (SYM-H) and asymmetric (ASYM-H) horizontal components of magnetic measurement, the solar wind temperature and the dynamic pressure (P) for the period of 1 – 31 March 2015. The 17 March, 2015 is characterized by a dramatic enhancement of ring current (indicated by H-component of the geomagnetic field) which is a unique feature of coronal mass ejections (CMEs)-driven storms (Pokhotelov et al., 2009). The storm activity started after the CMEs that was produced by long duration C9 solar flare hit the Earth (Borries et al., 2016). Its arrival generated a storm sudden commencement (SSC), which occurred on 17 March 2015 and its signature is observed by the sudden increased in value of the SYM-H around that period. During this period, SYM-H recorded it maximum value of ~70 nT, V_z increased from ~400 km to ~500 km and IMF- B_z also increased from ~5 nT to ~25 nT northward. The gradual decreased in the value of SYM-H up to about -100 nT on 17 March marked the beginning of the first sub-storm. There is a partial recovery between the first and second sub-storms. This partial recovery occurred between 09:30 UT – 12:00 UT (Yadav et al. 2016). The second sub-storm is characterized by long duration of southward orientation with a short-lived

northward fluctuation in-between before returning back to its normal condition. Again, SYM-H decreased further until its minimum value is attained, the values of A_p and K_p also increased to a maximum of 180 and 8 respectively. Although the recovery phase lasted for over 7 days, in this study, we only examine the effect of this storm activity on the development of ionospheric irregularities during the main phase (17 March 2015) and a day after (18 March 2015).

The plots in Figs. 8 - 11 show the variation of ROTI during the disturbed days (17 – 18 March, 2015) against the monthly average behaviors for the different sectors. We have extended the plots in the American sector to some hours on the 19 March in order to capture the irregularities during the first day following the recovery of the storm. The results obtained reveal significant longitudinal differences in the occurrence of ionospheric irregularities during the disturbed geomagnetic condition. At the American sector, ionospheric irregularities exhibit wide range of variations such as enhancement/suppression in the strength of irregularities, shift in the time of its occurrence and a significant longitudinal variation within the same sector. During the night following the main phase, the storm appeared not to have hindered the development of irregularities in all the stations in the American sector. Generally, a slight enhancement in the strength relative to the quiet-time values was observed in most of the stations as well as a shift in the time of occurrence. Its appearance is earlier at SAVO and BOGT (a double peak structure) and was registered later around the local post-midnight hours at RIOP. However, the observation during the first night following the recovery of the storm is quite different. Irregularities were noted at SAVO (long. $\sim 39^\circ\text{W}$) and KOUG (long. $\sim 53^\circ\text{W}$) and is absent at BOGT (long. $\sim 74^\circ\text{W}$) and RIOP (long. $\sim 79^\circ\text{W}$). This indicates a significant longitudinal variation within the American sector. The observation during the main phase of the storm can be partly attributed to the storm timing. The storm main phase occurred between the local mid-night hours and the post-sunset period in the American sector. The penetration of electric field around this period may not have hindered the occurrence but may rather favor it. It is well known that the Rayleigh-Taylor (R-T) and plasma density instabilities that cause the development of irregularities in the ionosphere are affected by some external driving forces such as electric fields, the magnetic field and neutral wind (Li et al., 2011). Due to the uniqueness of the magnetic orientation at the equatorial region, the ionosphere at the equatorial region is sensitive to any change in electric field. During geomagnetic storms, strong electric field which originate from the magnetosphere can penetrate down to the low latitudes (Buonsanto, 1999). An eastward (or westward) electric field during the daytime may favor (or impede) the upward drift of plasma. The injection of the eastward electric field during the main phase may have intensified the normal upward plasma drift and may have favored the development of irregularities. Increase in the height of the peak height of the F2-layer (h_mF_2) relative to the reference quiet day average values were among the different observations reported by Kuai et al. (2016) over the American sector due to the multiple action of penetration electric fields (PEFs) of the 17 March 2015 storm event. Increase in h_mF_2 due to PEFs ensures sharper density gradient; a condition that may favor the development of irregularities. The slight enhancement in the strength of the irregularities may be an indication that the h_mF_2 height due to storm-induced electric field is higher than the reference quiet-time drift.

On the other hand, the observations during the first night following the recovery of the storm can be explained in terms of the longitudinal differences in the action of storm induced disturbance dynamo mechanism. Previous investigations of the 17 March 2015 storm event have reported a notable longitudinal variation in the storm-induced thermospheric wind circulation. Zhang et al. (2015) has reported a significant poleward surge in thermospheric wind at the mid and subauroral latitudes in the

American sector following the 17 March storm event. Tulasi Ram et al. [2015] on the hand reported an equatorward thermospheric wind in the Asian longitudes. The action of poleward wind following this storm event had been reported by Zhang et al. (2015) to have prevented the equatorward wind in the American sector with a consequence failure of storm-induced disturbance dynamo mechanism at the equatorial region. This scenario may favor the occurrence of irregularities in the American sector depending on the day-to-day variability. However, in longitudes where there is equatorward thermospheric wind, storm-induced disturbance dynamo mechanism is inevitable and therefore there is possibility of inhibition of irregularities in the region due to the action of disturbance electric fields. In this study, irregularities are observed along the meridians $\sim 39^\circ\text{W}$ (SAVO) and $\sim 53^\circ\text{W}$ (KUG) and absent long. $\sim 74^\circ\text{W}$ (BOGT) and $\sim 79^\circ\text{W}$ (RIOP) on the first night following the storm's recovery. This may suggest that the regional circulation background that may prevent the development of disturbance dynamo mechanism at the low latitude suggested by Zhang et al. (2015) may not have affected the entire longitudes in the American sector but rather is confined to some longitudes. Although Hairston et al. (2016) suggested the possibility of the circulation not reaching the equator earlier, probably in some longitude. Our observed longitudinal variation within the American sector is similar to what Rajesh et al. (2017) and Patra et al. (2016) reported over the Asian sector during this storm event.

The scenario in the African sector is quite different compared to the observations in the American sector.

The storm activity appeared to have hindered the development of irregularities on both days (i.e. during the storm's main phase and the first night following the recovery phase) as observed in Fig 9. The PEFs, which is injected into the low latitude during the main phase of the storm had occurred between the local sunrise hour sector and around the post mid-night hour: a time which may not have favored the occurrence of irregularities in the African sector. The injection of PEFs may have inhibited the diffusion of plasma that might have caused plasma instability with a consequence failure of occurrence of irregularities.

Also, the inhibition of irregularities that was observed on the first night of recovery day (18th March 2015) in the African sector may be an indication of the effect of other storm induced related drivers whose action may produce a mechanism that may not favor the upward motion of plasma. Such drivers may include the action of a westward (i) PEFs due to northward orientation of Bz during the recovery phase and (ii) disturbance dynamo electric field due to storm induced equatorward wind. In this storm event, the Bz northward orientation associated with the storm recovery is short-lived and it occurred between the local post-midnight hours and the dawn in African longitude, therefore case (i) may be ruled out. The inhibition of irregularities in all the stations in the African region may be an evidence of the disturbance dynamo mechanism on the 18th March 2015 in Africa equatorial region; a development that is fundamentally similar to some longitudes in the America sector where irregularities is absent on the first night following the storm recovery. Since irregularities is absent in all the stations during this period, this may suggest that the action of disturbance dynamo mechanism may not be restricted to some longitude within the region.

Further, it can be observed that irregularities are absent at Asian and Oceania longitudes during the two storm days as shown in Figs. 10 and 11. The weak and irregular structure of irregularities observed at the Asian sector during the quiet condition, particularly at PBR2, were completely absent during the two disturbed days. Although, Rajesh et al. (2017) and many other authors that investigated the ionospheric irregularities dynamics during this storm observed the occurrence of irregularities over the

Indian region, however, Patra et al. (2016) has reported the confinement of plasma bubbles and irregularities to a narrow longitude of 69° - 98° E. This was also confirmed in the investigations this storm event by Carter et al. (2016) and Rajesh et al. (2017). Rajesh et al. (2017) had found that irregularities occurred in the Indian longitude and is absent in Taiwan both in the Asian sector. This may also explain why irregularities are absent at Thailand (CUSV) and Indonesia (BAKO and BTNG).

On the contrary, PBR2 is a station within the longitudinal range reported by Patra et al. (2016) and no irregularities was observed during the storm event. Although no plausible explanation can be given, however, we suggest latitudinal difference in the variation between the station used by Patra et al. (2016) and PBR2. Patra et al. (2016) had used a station located outside the electrojet belt (Gadanki: 13.5° N, 79.2° E, Mag. lat. 6.5° N), while in this case PBR2 is located at the flank of the electrojet which could cause a significant variation.

Conclusion

We have investigated the dynamics of ionospheric irregularities at different sectors during the month of March 2015. This month consists of a period of both quiet and disturbed ionospheric conditions. We found that during quiet geomagnetic condition, severe irregularities are prominent only in the American and African sectors and are rarely observed at the Oceania and Asian sectors. The strength is however found to decrease eastward. This has been attributed to the eastward decrease in equatorial electrojet current around the post-sunset period or a westward decrease in counter electrojet current around the same hours during the period under investigation. Further investigation using observations from array of magnetometers placed along the different longitudes may help to ascertain which of the drivers is responsible for the eastward decreases in the strength of irregularities. We also found that the occurrence of irregularities during the 17 March 2015 storm event differs from one sector to another. Irregularities are found to be present in all the stations in the American longitude during the night following the main phase. However, significant longitudinal variation was observed within the sector during the first night following the storm's recovery. This development may suggest a notable longitudinal difference in the effect of storm-induced disturbance dynamo mechanism within the American sector. We also found that irregularities are absent in all the stations in the African, Asian and Oceania longitudes during the storm periods. This development is opposite the normal average quiet day characteristics in African sector: a possibility of suppression or cancellation of normal quiet day pre-reversal enhancement in the African region owing to the action of storm-induced associated fields. Also, the observation in the African sector suggests that the effect of the disturbance dynamo mechanism may not be confined to some longitudes within the region as observed in the American sector but rather affects the entire longitudes. This investigation also confirms that in studying the effect of storm activity on occurrence of irregularities, it is essential to consider the effect due to storm timing and also differentiate between the local, region and global characteristics.

Acknowledgement

The authors are grateful to the International GNSS Service (IGS) community for granting access to their database available at <ftp://geodaf.mt.asi.it/GEOD/GPSD/RINEX>. We thank the scientists at various IGS stations whose data were used for this study for the continued availability of GPS data.

References

- Aaron, J. and S. Basu, (1994), Ionospheric amplitude and phase fluctuations at the GPS frequencies, Proceedings of ION GPS 94, 1569-1578

- 319 Aarons, J. (1991), The role of the ring current in the generation or inhibition of equatorial F-layer
320 irregularities during magnetic storms, *Radio Sci.*, 26, 1131-1149.
- 321 Aarons, J. (1993), The longitudinal morphology of equatorial F-layer irregularities relevant to their
322 occurrence, *Space Sci. Rev.*, 63, 209–243.
- 323 Abdu, M., I. Batista, and J. Bittencourt, (1981), Some characteristics of spread-F at the magnetic
324 equatorial station Fortaleza, *J. Geophys. Res.*, 86, 6836–6842, 1981.
- 325 Basu, S., E. MacKenzie, and Su. Basu, (1988), Ionospheric constraints on VHF/UHF communications
326 links during solar maximum and minimum periods, *Radio Sci.* 23 (3), 363–378.
- 327 Basu, Su, and S. Basu, (1985), Equatorial scintillations: advances since ISEA-6, *J. Atmos. Terr. Phys.*
328 47 (8), 753–768.
- 329 Biktash, L.Z., (2004), Role of the magnetospheric and ionospheric currents in the generation of the
330 equatorial scintillations during geomagnetic storms, *Annales Geophysicae*, 22, 3195-3202.
- 331 Borries, C., Mahrous, A. M., Ellahouny, N. M., and R. Badeke, (2016), Multiple Ionospheric
332 Perturbations during the Saint Patrick's Day Storm 2015 in the European-African Sector, *J.*
333 *Geophys. Res. Space Physics*, doi: 10.1002/2016JA023178
- 334 Buonsanto M.J., (1999), 'Ionospheric Storm – A review', *Space Science Reviews*, 88, 563-601.
- 335 Campos de Rezende, L.F., E. Rodrigues de Paula, I. Stacarini Batista, I. Jelinek Kantor and M. Tadeu
336 de Assis Honorato Muella, (2007), Study of Ionospheric irregularities during intense magnetic
337 storm, *Revista Brasileira de Geofisica*, 25 (2), 151-158.
- 338 Carter, B. A., E. Yizengaw, R. Pradipta, J. M. Retterer, K. Groves, C. Valladares, R. Caton, C.
339 Bridgwood, R. Norman, and K. Zhang (2016), Global equatorial plasma bubble occurrence
340 during the 2015 St. Patrick's Day storm, *J. Geophys. Res. Space Physics*, 121, 894-905,
341 doi:10.1002/2015JA022194.
- 342 Chu, F. D., J. Y. Liu, H. Takahashi, J. H. A. Sobral, M. J. Taylor and A. F. Medeiros, (2005), The
343 climatology of ionospheric plasma bubbles and irregularities over Brazil, *Annales Geophysicae*,
344 23, 379-384.
- 345 Deng B., J. Huang, D. Kong, J. Xu, D. Wan, and G. Lin, (2015), Temporal and spatial distributions of
346 TEC depletions with scintillations and ROTI over south China, *Advances in Space Research*, 55,
347 259–268.
- 348 Fejer, B. G., L. Scherliess, and E. R. de Paula, (1999), Effects of the vertical plasma drift velocity on
349 the generation and evolution of equatorial spread F, *J. Geophys. Res.*, 104(A9), 19, 859–19,869,
350 doi:10.1029/ 1999JA900271.
- 351 Hairston, M., W. R. Coley, and R. Stoneback (2016), Responses in the polar and equatorial ionosphere
352 to the March 2015 St. Patrick Day storm, *J. Geophys. Res. Space Physics*, 121, 11,213–11,234,
353 doi:10.1002/2016JA023165.

- Huang, C.-S., G. R. Wilson, M. R. Hairston, Y. Zhang, W. Wang, and J. Liu (2016), Equatorial ionospheric plasma drifts and O⁺ concentration enhancements associated with disturbance dynamo during the 2015 St. Patrick's Day magnetic storm, *J. Geophys. Res. Space Physics*, 121, 7961–7973, doi:10.1002/2016JA023072.
- Huba, J.D., S. Sazykin, and A. Coster, (2016), SAMI3-RCM Simulation of the March 17, 2015 Geomagnetic Storm, *J. Geophys. Res. Space Physics*, doi: 10.1002/2016JA023341.
- Hysell, D. L. and J. Burcham, (1998), JULIA radar studies of equatorial spread-F, *J. Geophys. Res.*, 103, 29155–29167.
- Ikubanni, S.O, Adebisi, S.J, Adebisin, B.O, Dopamu, K.O, Joshua, B.W, Bolaji, O.S and B.J. Adekoya (2018), Response of Gps-Tec in the African Equatorial Region to the Two Recent St. Patrick's Day Storms, *International Journal of Civil Engineering and Technology*, 9(10), 1773–1790.
- Kil, H., W. K. Lee, L. J. Paxton, M. R. Hairston, and G. Jee (2016), Equatorial broad plasma depletions associated with the evening prereversal enhancement and plasma bubbles during the 17 March 2015 storm, *J. Geophys. Res. Space Physics*, 121, 10,209–10,219, doi:10.1002/2016JA023335.
- Kintner P.M., B.M. Ledvina, and De paula, (2007), GPS and Ionospheric Scintillations, *Space Weather*, 5, S09003, doi:10.1029/ 2006SW000260.
- Kuai, J., L. Liu, J. Liu, S. Sripathi, B. Zhao, Y. Chen, H. Le, and L. Hu (2016), Effects of disturbed electric fields in the lowlatitude and equatorial ionosphere during the 2015 St. Patrick's Day storm, *J. Geophys. Res. Space Physics*, 121, doi:10.1002/2016JA022832.
- Li, G., B. Ning, M. A. Abdu, X. Yue, L. Liu, W. Wan, and L. Hu, (2011), On the occurrence of post-midnight equatorial F region irregularities during the June solstice, *J. Geophys. Res.*, 116, A04318, doi: 101029/2010JA016056.
- Li, G., B. Ning, W. Wan and B. Zhao, (2006), Observations of GPS ionospheric scintillations over Wuhan during geomagnetic storms, *Annales Geophysicae*, 24, 1581-1590.
- Li, G., B. Ning, B. Zhao, L. Liua, J. Y. Liu and K. Yumoto, (2008), Effects of geomagnetic storm on GPS ionospheric scintillations at Sanya, *J. Atmos. Sol. Terr. Phys.*, 70, 1034-1045.
- Lynn, K., Y. Otsuka, and K. Shiokawa, (2011), Simultaneous observations at Darwin of equatorial bubbles by ionosonde-based range/time displays and airglow imaging, *Geophys. Res. Lett.*, 38, L23101, doi:10.1029/2011GL049856.
- Mendillo, M., B. Lin, and J. Aarons, (2000), The application of GPS observations to equatorial aeronomy, *Radio Sci.*, 35, 885–904.
- Muella, M.T.A.H., E.R. de Paula, Kantor, I.J., Rezende, L.F.C., and P.F. Smorigo, (2009), Occurrence and zonal drifts of small-scale ionospheric irregularities over an equatorial station during solar maximum – magnetic quiet and disturbed conditions, *Adv. Space Res.* 43, 1957–1973.

- 390 Nava, B., Rodríguez-Zuluaga, J., Alazo-Cuartas, K., Kashcheyev, A., Migoya-Orué, Y., Radicella,
391 S.M., Amory-Mazaudier, C., and R. Fleury, (2016), Middle- and low-latitude ionosphere
392 response to 2015 St. Patrick's Day geomagnetic storm, *J. Geophys. Res. Space Physics*,
393 <https://doi.org/10.1002/2015JA022299>.
- 394 Ngwira, C.M., G.K. Seemala, and J.B. Habarulema, (2013), Simultaneous observations of ionospheric
395 irregularities in the African low-latitude region. *Journal of Atmospheric and Solar-Terrestrial*
396 *Physics* 97, 50–57.
- 397 Oladipo, O. A. and T. Schüler, (2013), Equatorial ionospheric irregularities using GPS TEC derived
398 index, *J. Atmos. Sol. Terr. Phys.*, 92, 78-82.
- 399 Oladipo, O. A. and T. Schüler, (2013), Magnetic storm effect on the occurrence of ionospheric
400 irregularities at an equatorial station in the African sector, *Annals of Geophysics*, 56, 5, 2013,
401 a0565; doi:10.4401/ag-6247 a0565.
- 402 Patra, A. K., P. P. Chaitanya, N. Dashora, M. Sivakandan, and A. Taori (2016), Highly localized
403 unique electrodynamics and plasma irregularities linked with the 17 March 2015 severe
404 magnetic storm observed using multi technique common-volume observations from Gadanki,
405 India, *J. Geophys. Res. Space Physics*, 121, 11,518–11,527, doi:10.1002/2016JA023384.
- 406 Patra, A. K., P. P. Chaitanya, N. Dashora, M. Sivakandan, and A. Taori (2016), Highly localized
407 unique electrodynamics and plasma irregularities linked with the 17 March 2015 severe
408 magnetic storm observed using multitechnique common-volume observations from Gadanki,
409 India, *J. Geophys. Res. Space Physics*, 121, 11,518–11,527, doi:10.1002/2016JA023384.
- 410 Pi, X., A.J. Mannucci, U.J. Lindqwister, and C.M. Ho, (1997), Monitoring of global ionospheric
411 irregularities using the worldwide GPS network, *Geophysical Research Letters*, 24, 2283–2286.
- 412 **Pokhotelov, D., Mitchell, C. N., Jayachandran, P. T., MacDougall, J. W. and M. H. Denton**
413 **(2009), Ionospheric response to the corotating interaction region–driven geomagnetic**
414 **storm of October 2002, *J. Geophys. Res.*, 114, A12311, doi:10.1029/2009JA014216.**
- 415 Ray, S., B. Roy, K. S. Paul, S. Goswami, C. Oikonomou, H. Haralambous, B. Chandel, and A. Paul
416 (2017), Study of the effect of March 17–18, 2015 geomagnetic storm on the Indian longitudes
417 using GPS and C/NOFS, *J. Geophys. Res. Space Physics*, 122, 2551–2563,
418 doi:10.1002/2016JA023127.
- 419 Spogli, L., et al. (2016), Formation of ionospheric irregularities over Southeast Asia during the 2015
420 St. Patrick's Day storm, *J. Geophys. Res. Space Physics*, 121, 12,211–12,233,
421 doi:10.1002/2016JA023222.
- 422 Su, S. Y., C. K. Chao, C. H. and Liu, (2008), On monthly/seasonal/longitudinal variations of equatorial
423 irregularity occurrences and their relationship with the post-sunset vertical drift velocities, *J.*
424 *Geophys. Res.*, 113, A05307, doi:10.1029/2007ja012809.
- 425 Tanna, H.J., and K.N. Pathak, (2014), Longitude dependent response of the GPS derived ionospheric
426 ROTI to geomagnetic storms, *Astrophys. Space Sci.*, 350, 47–56.

- 427 Tulasi Ram, S., et al. (2015), Duskside enhancement of equatorial zonal electric field response to
 428 convection electric fields during St. Patrick's Day storm on 17 March 2015, *J. Geophys. Res.*
 429 *Space Physics*, 120, doi:10.1002/2015JA021932.
- 430 Woodman, R.F. and C. LaHoz, (1976), Radar observations of F region equatorial irregularities, *J.*
 431 *Geophys. Res.*, 81, pp.5447-5466.
- 432 Yadav, S., S. Sunda, and R. Sridharan (2016), The impact of the 17 March 2015 St. Patrick's Day
 433 storm on the evolutionary pattern of equatorial ionization anomaly over the Indian longitudes
 434 using high-resolution spatiotemporal TEC maps: New insights, *Space Weather*, 14,
 435 doi:10.1002/2016SW001408.
- 436 Yeh, K.C., and C.H. Liu, (1982), Radio wave scintillations in the ionosphere, *Proceedings of IEEE*, 70,
 437 324–360.
- 438 Zhang, S.-R., et al. (2015), Thermospheric poleward wind surge at midlatitudes during great storm
 439 intervals, *Geophys. Res. Lett.*, 42, 5132–5140, doi:10.1002/2015GL064836.
- 440 Zhang, S.-R., Y. Zhang, W. Wang, and O. P. Verkhoglyadova (2017), Geospace system responses to
 441 the St. Patrick's Day storms in 2013 and 2015, *J. Geophys. Res. Space Physics*, 122,
 442 doi:10.1002/2017JA024232.
- 443 Zhou, Y.-L., H. Lüher, C. Xiong, and R. F. Pfaff (2016), Ionospheric storm effects and equatorial
 444 plasma irregularities during the 17–18 March 2015 event, *J. Geophys. Res. Space Physics*, 121,
 445 9146–9163, doi:10.1002/2016JA023122.

Fig. 1: Map of the world showing the location of the stations used.

Fig.2: Diurnal plots of the average ROTI values at different stations in the South American sector during the period 01-31 March, 2015.

Fig. 3: Diurnal plots of the average ROTI values at different stations in the African sector during the period 01-31 March, 2015.

Fig. 4: Diurnal plots of the average ROTI values at different stations in the Asian sector during the period 01-31 March, 2015.

Fig. 5: Diurnal plots of the average ROTI values at different stations over the Oceania during the period 01-31 March, 2015.

Fig. 6: The average quiet-time variation of ROTI at all the stations for the month of March, 2015

Fig. 7: Variability of (a) the interplanetary magnetic field B_z and (b) B_y components, (c) the planetary A_p and (d) K_p indices, (e) the proton density (N_p), (f) the solar wind speed, (g) the symmetric (SYM-H) and (h) asymmetric (ASYM-H) horizontal components of magnetic measurement, (i) the solar wind temperature and (j) the solar wind dynamic pressure (P) for the period of 1 – 31 March 2015.

Fig. 8: Variation of ROTI_{ave} in South American sector during the storm days of 17 -19 March, 2015 and the average quiet-time variation of ROTI for the same month.

Fig. 9: Variation of ROTI_{ave} in the African sector during the storm days of 17 -18 March, 2015 and the average quiet-time variation of ROTI for the same month.

Fig.10: Variation of ROTI_{ave} in the Asian sector during the storm days of 17 -18 March, 2015 and the average quiet-time variation of ROTI for the same month.

Fig.11: Variation of ROTI_{ave} in the Oceania sector during the storm days of 17 -18 March, 2015 and the average quiet-time variation of ROTI for the same month.

Table1: Geophysical details of the IGS stations used.

Location	Country	Station Code	Geographic		Geomagnetic		Time (LT)
			Lat.	Long.	Lat.	Long.	
American Sector							
Salvador	Brazil	SAVO	-12.97	-38.50	4.22	110.11	LT = UT - 3 h
Bogota	Colombia	BOGT	4.71	-74.07	-3.76	146.60	LT = UT - 5 h
French Guiana		KOUG	3.93	-53.12	-4.10	124.94	LT = UT - 3 h
Riobamba	Ecuador	RIOP	-1.66	-78.65	-10.98	149.77	LT = UT - 5 h
African Sector							
Dakar	Senegal	DAKR	14.76	-17.36	3.12	-89.08	LT = UT
Addis Ababa	Ethiopia	ADIS	8.98	38.75	0.11	110.45	LT UT + 3 h
Yamoussoukro	Coted'ivore	YKRO	6.82	-5.28	-2.89	77.26	LT = UT
Cotonou	Benin Rep.	BJCO	6.37	2.39	-3.08	74.48	LT = UT
Malinda	Kenya	MAL2	-3.21	40.11	-12.66	111.77	LT = UT + 3 h
Asian Sector							
Patumwan	Thailand	CUSV	13.74	100.53	5.81	172.10	LT = UT +7 h
Port Blair	India	PBR2	11.64	92.71	3.41	164.40	LT = UT +6 h
Cibinong	Indonesia	BAKO	-6.49	106.85	-1.86	178.28	LT = UT +7 h
Bitung	Indonesia	BTNG	1.48	125.19	-6.87	196.41	LT = UT + 8 h
Oceania Sector							
Kiribati	Betio	KIRI	1.35	172.92	-2.32	244.39	LT = UT + 12 h
Tuvalu	Funafuti	TUVA	-7.10	177.64	9.98	250.61	LT = UT + 12 h
Yaren District	Nauru	NAUR	-0.55	166.53	-4.42	238.61	LT = UT + 11 h

F

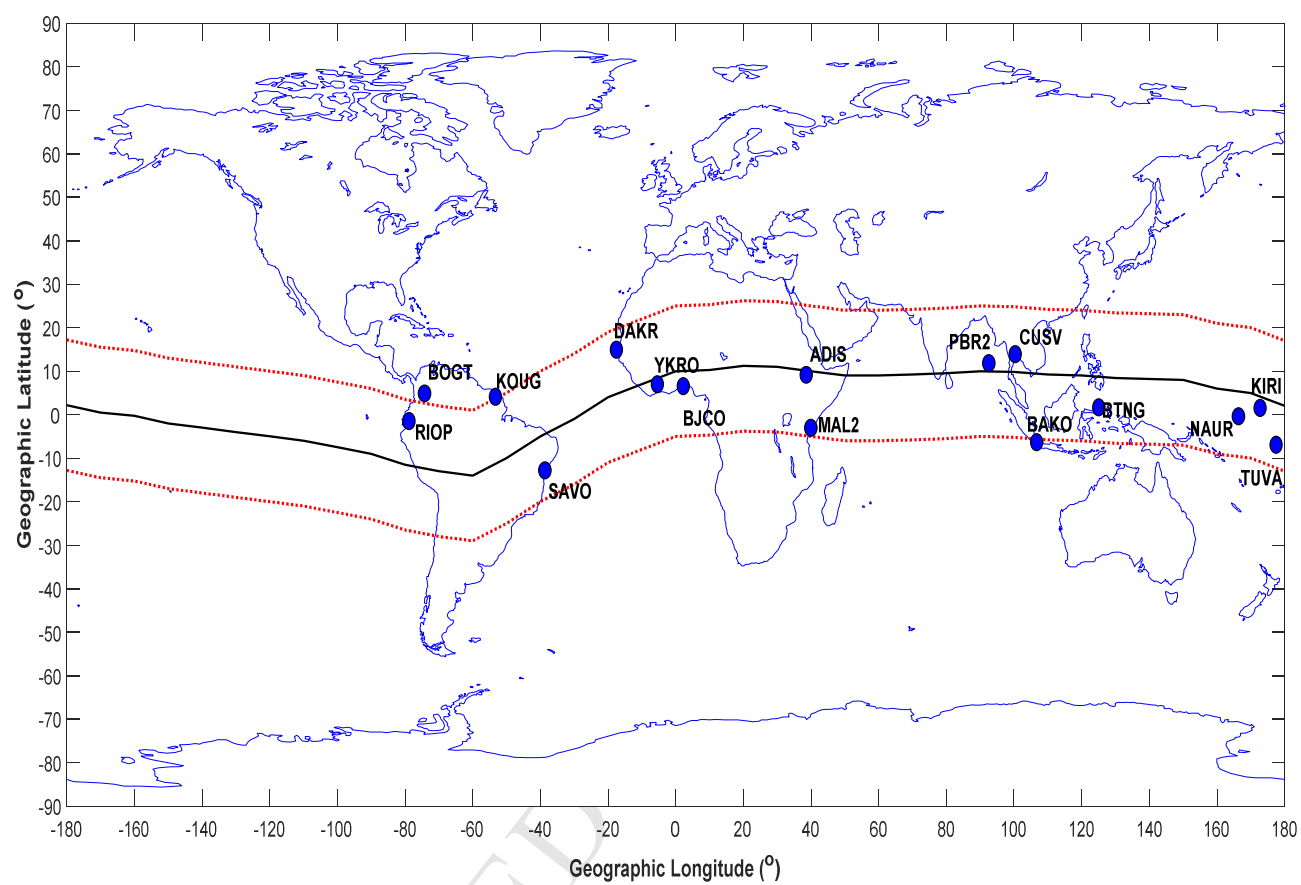


Fig. 1

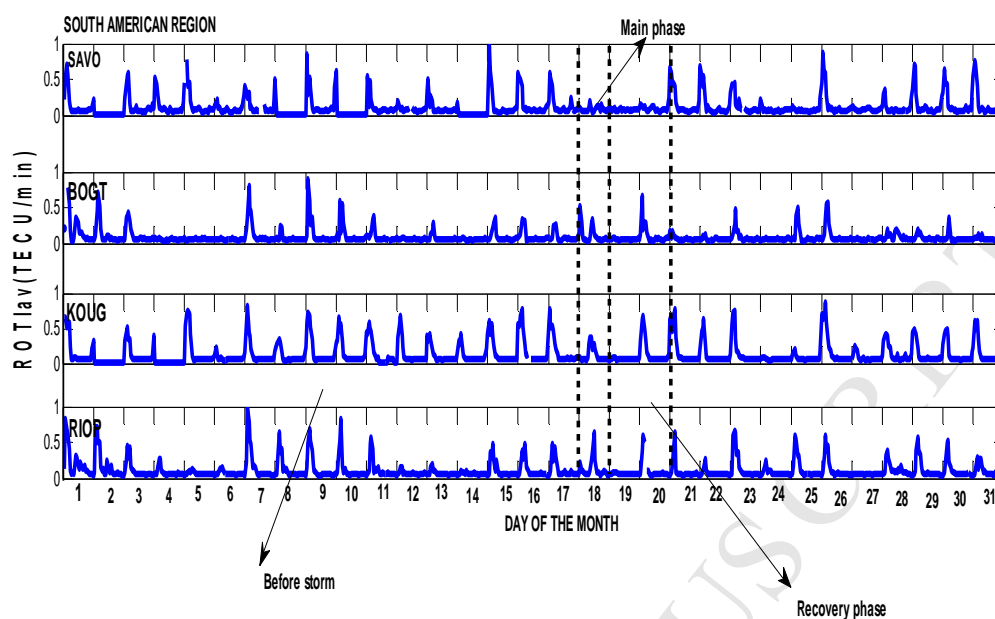


Fig.2

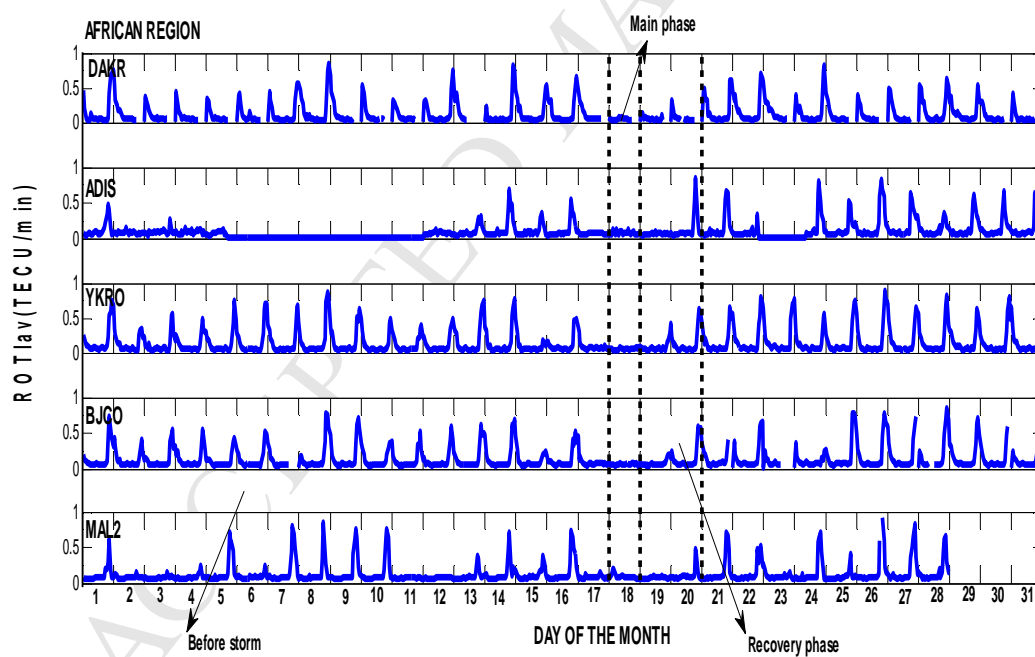


Fig. 3

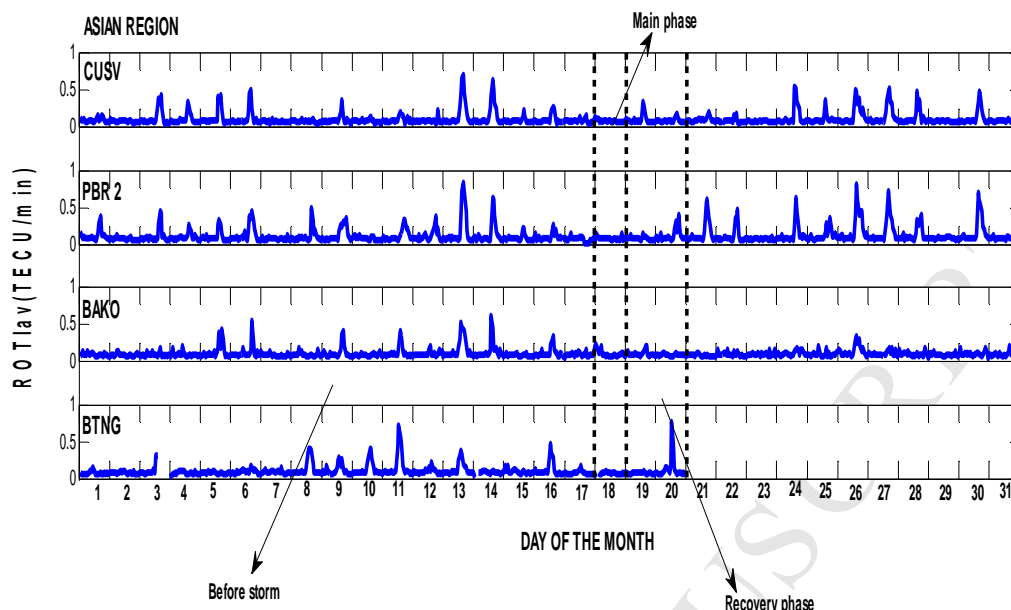


Fig. 4

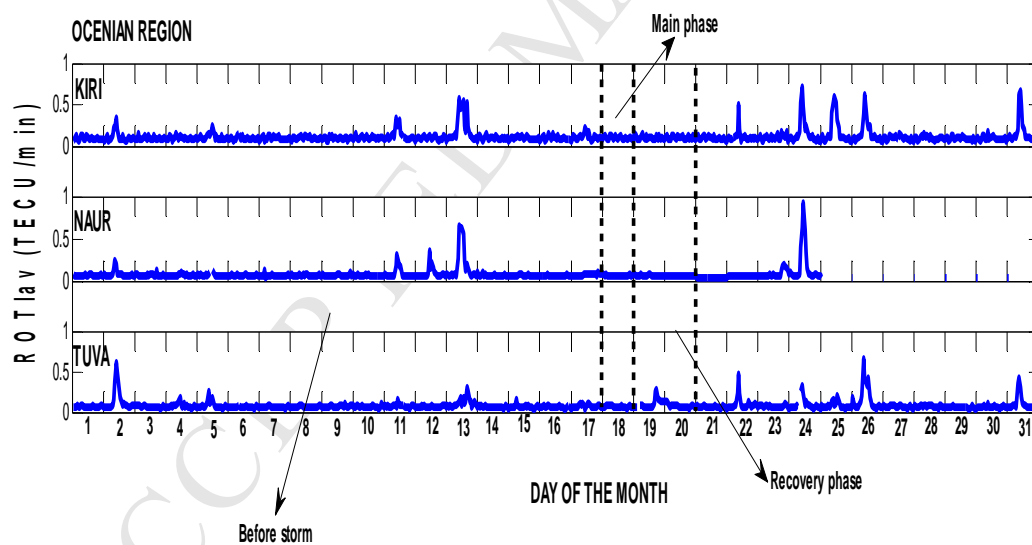


Fig. 5

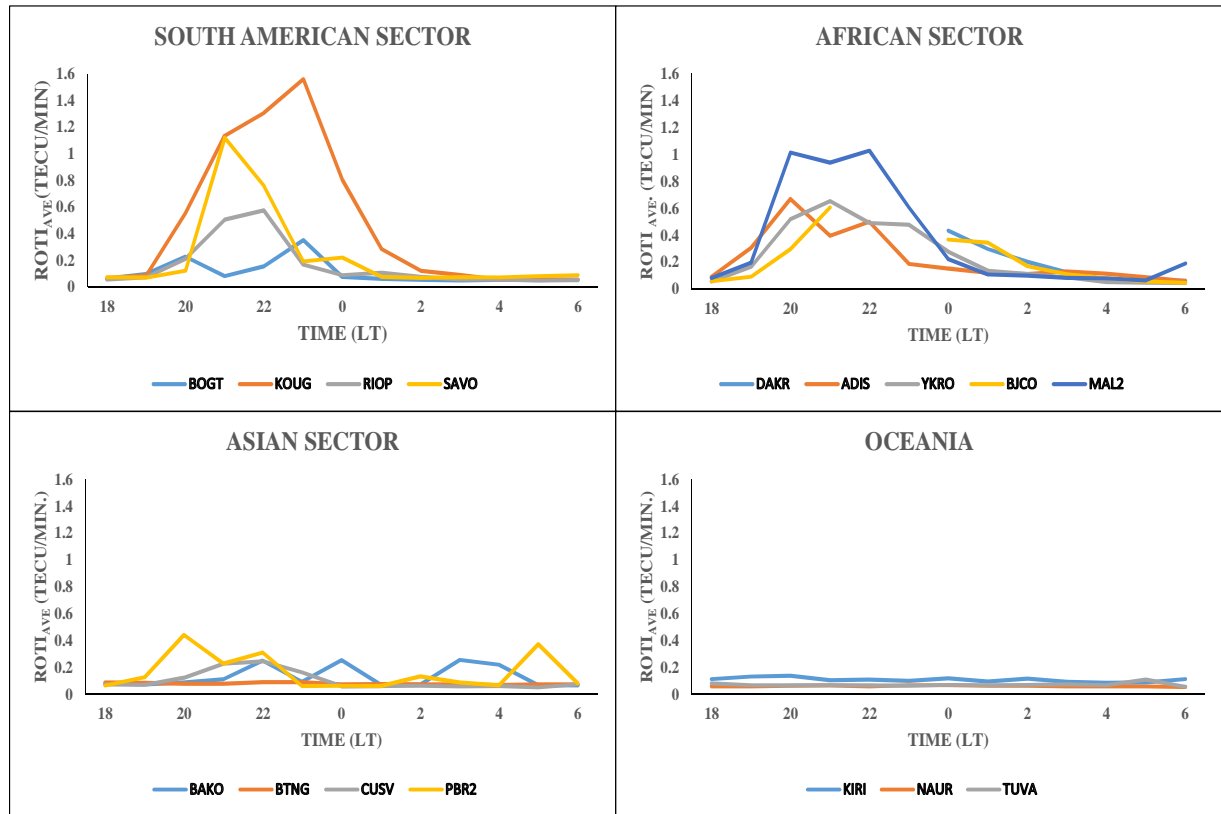


Fig. 6: The average quiet-time variation of ROTI at all the stations for the month of March, 2015.

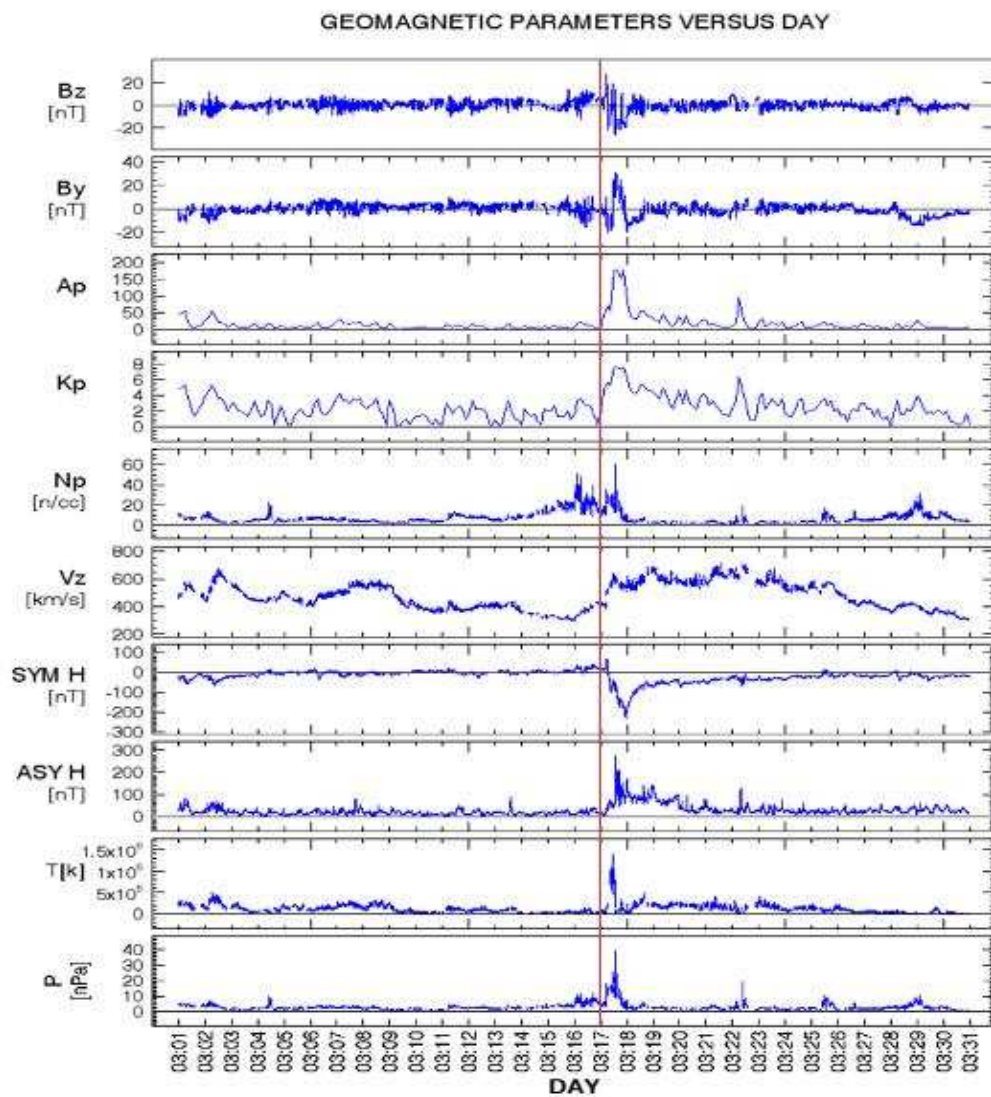


Fig. 7

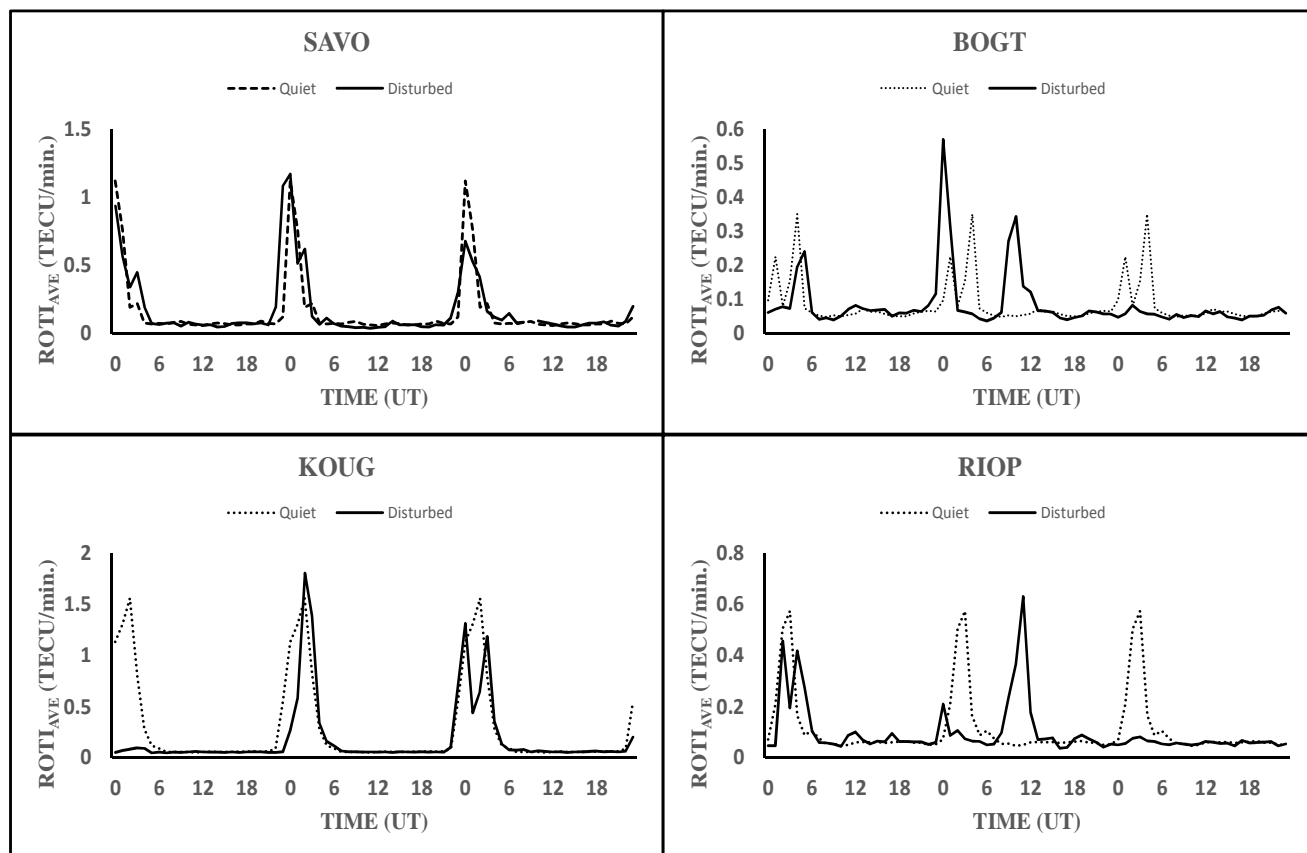


Fig. 8

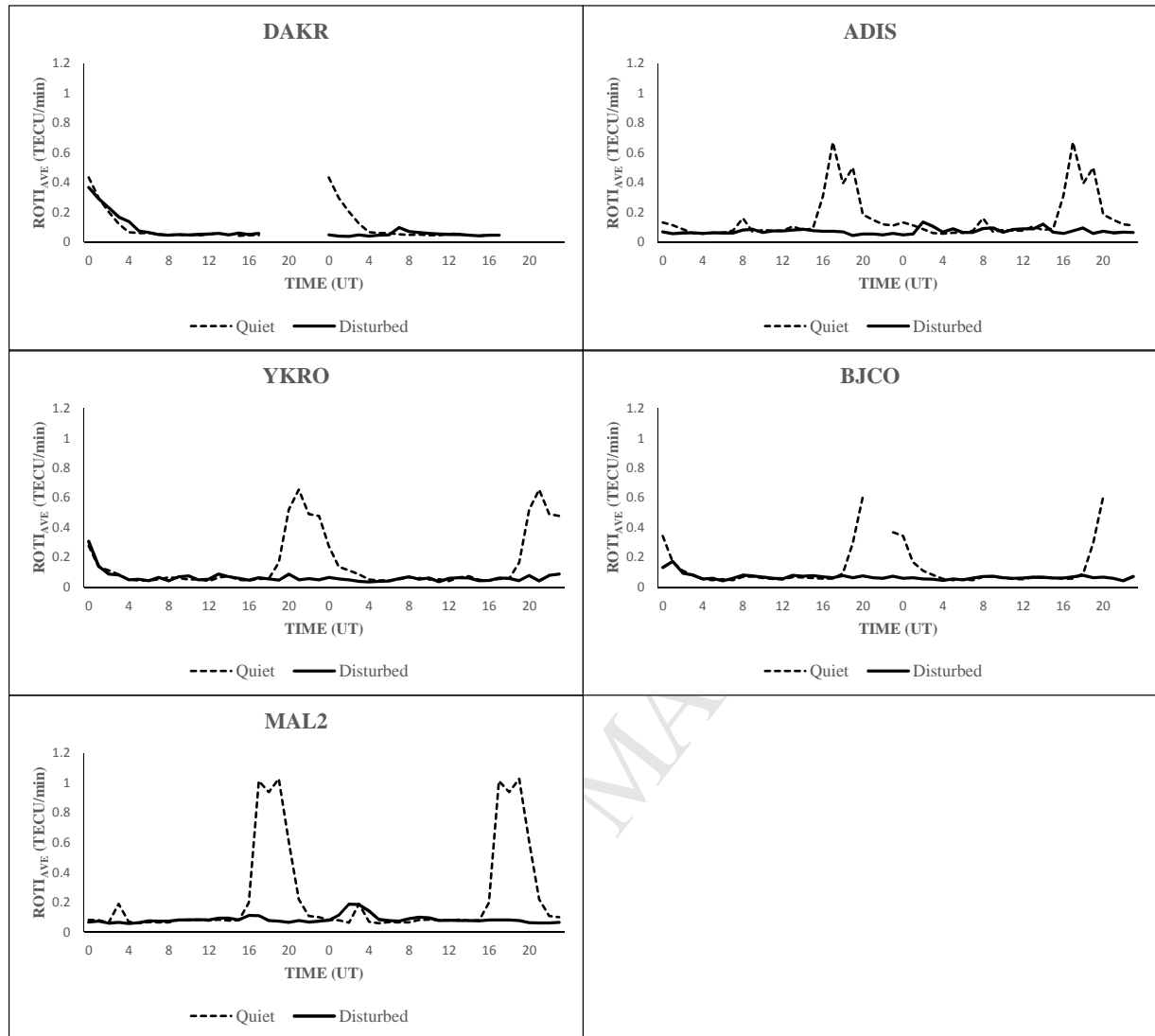


Fig. 9

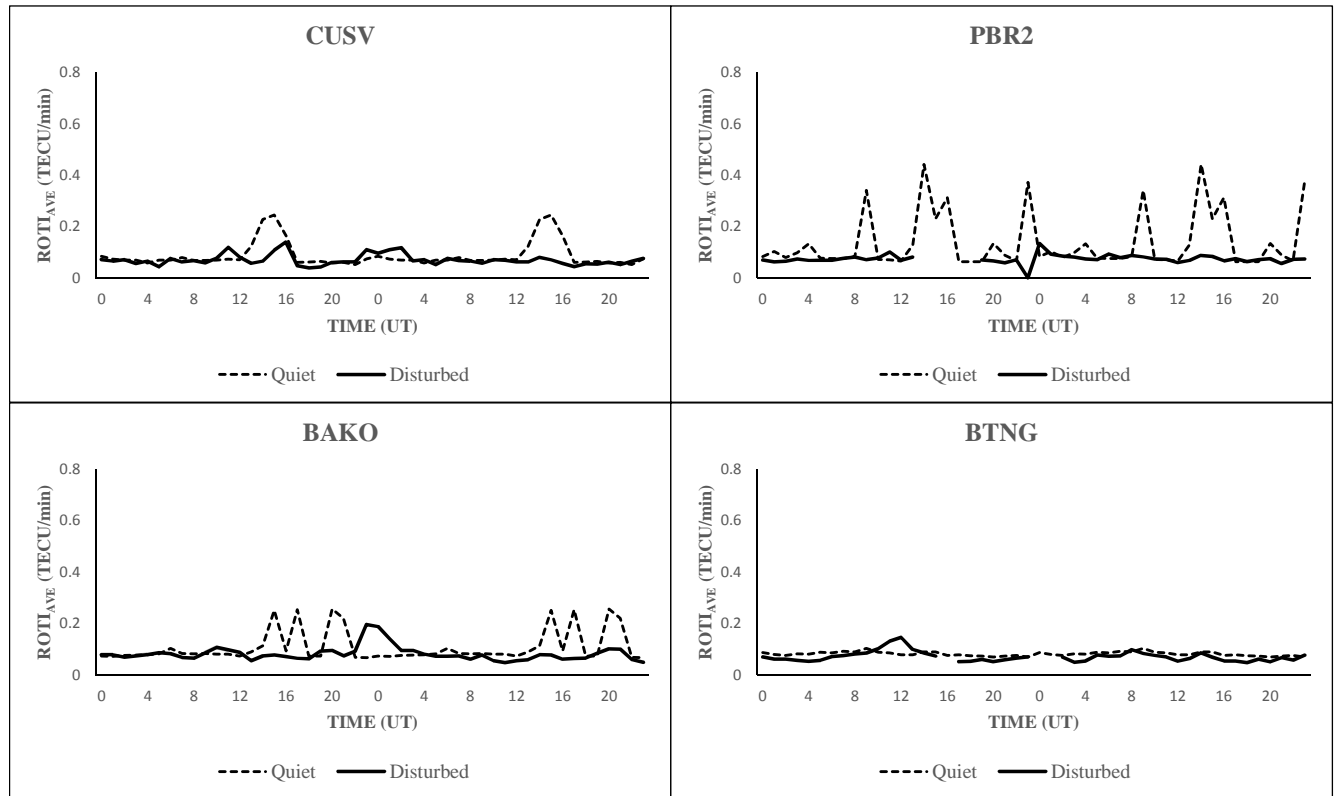


Fig. 10:

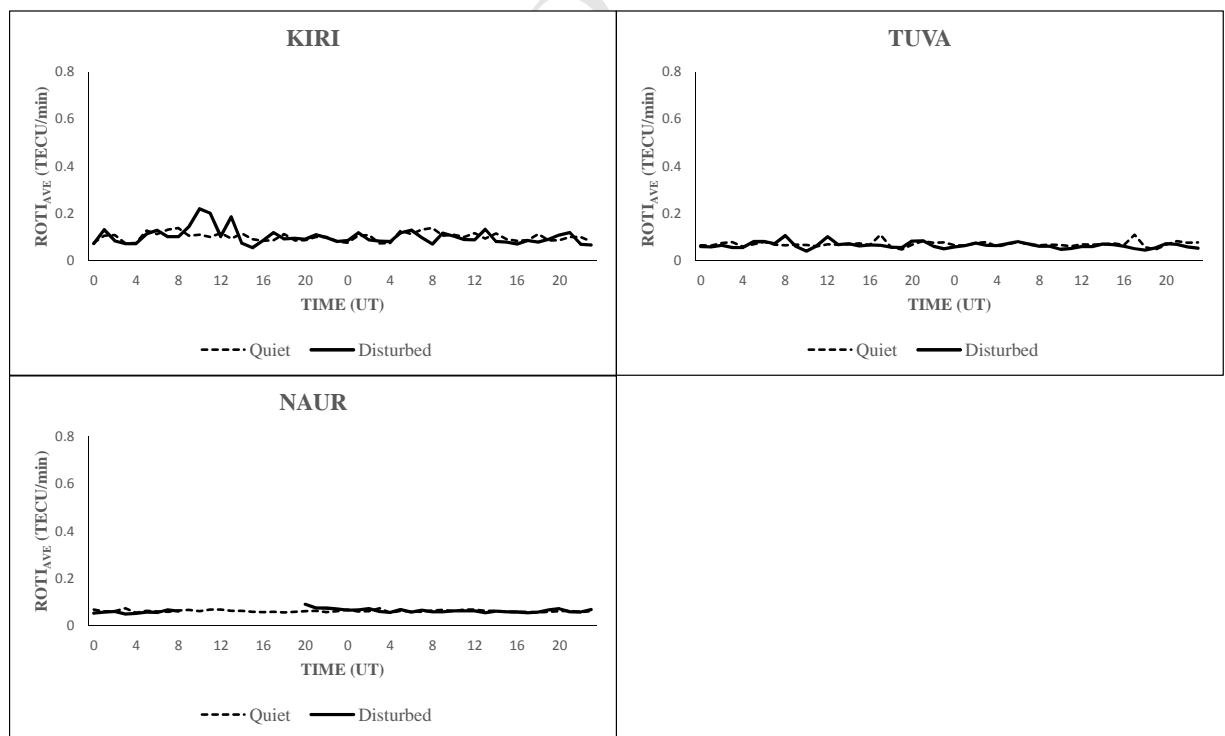


Fig. 11

Highlights

- The magnitude of irregularities decreases from eastward for quiet-time condition.
- Notable longitudinal variations of irregularities during the 17 March 2015 storm.
- The storm-induced drivers and storm timing play major roles during the storm event.